

# Digits and fin rays share common developmental histories

Tetsuya Nakamura<sup>1\*</sup>, Andrew R. Gehrke<sup>1\*</sup>, Justin Lemberg<sup>1</sup>, Julie Szymaszek<sup>1</sup> & Neil H. Shubin<sup>1</sup>

**Understanding the evolutionary transformation of fish fins into tetrapod limbs is a fundamental problem in biology<sup>1</sup>. The search for antecedents of tetrapod digits in fish has remained controversial because the distal skeletons of limbs and fins differ structurally, developmentally, and histologically<sup>2,3</sup>. Moreover, comparisons of fins with limbs have been limited by a relative paucity of data on the cellular and molecular processes underlying the development of the fin skeleton. Here, we provide a functional analysis, using CRISPR/Cas9 and fate mapping, of 5' *hox* genes and enhancers in zebrafish that are indispensable for the development of the wrists and digits of tetrapods<sup>4,5</sup>. We show that cells marked by the activity of an autopodial *hoxa13* enhancer exclusively form elements of the fin fold, including the osteoblasts of the dermal rays. In *hox13* knockout fish, we find that a marked reduction and loss of fin rays is associated with an increased number of endochondral distal radials. These discoveries reveal a cellular and genetic connection between the fin rays of fish and the digits of tetrapods and suggest that digits originated via the transition of distal cellular fates.**

The origin of tetrapod limbs involved profound changes to the distal skeleton of fins. Fin skeletons are composed mostly of fin rays<sup>6</sup>, whereas digits are the major anatomical and functional components of the distal limb skeleton. One of the central shifts during the origin of limbs in the Devonian period involved the reduction of fin rays coincident with an expansion of the distal endochondral bones of the appendage<sup>2,7</sup>. Because the distal skeletons of fins and limbs are composed of different types of bone tissue (dermal and endochondral, respectively) it remains unclear how the terminal ends of fish and tetrapod appendages are related and, consequently, how digits arose developmentally. Although the understanding of ectodermal signalling centres in fin buds and fin folds has advanced in recent years<sup>8–11</sup>, that of the cells that form the skeletal patterns has remained elusive.

*Hox* genes, namely those of the *HoxA* and *HoxD* clusters, have figured prominently in discussions of limb development and origins<sup>3,12–14</sup>. The ‘early’ and ‘late’ phases of *HoxD* and *HoxA* transcription are involved in specifying the proximal (arm and forearm) and distal (autopod) segments, respectively<sup>15</sup>. Both fate map assays and knockout phenotypes in mouse limbs reveal an essential role for *Hox13* paralogues in the formation of the autopod<sup>4,5</sup>. Mice engineered to lack *Hoxa13* and *Hoxd13* in limbs lack the wrists and digits exclusively<sup>4</sup>. Moreover, the lineage of cells expressing *Hoxa13* resides exclusively in the autopod of adult mice<sup>5</sup>. Together, these lines of evidence reveal the extent to which 5' *Hox* genes are involved in, and serve as markers for, the developmental pattern of the wrist and digits. Unfortunately, as no such studies have yet been performed in fish, the means to find antecedents of autopodial development in fins has been lacking.

Analyses of 5' *Hox* expression in phylogenetically diverse wild-type fish<sup>16–19</sup> as well as experimental misexpression in teleosts reveal that 5' *Hox* activity may be involved in patterning<sup>20</sup>, and defining the extent of, the distal chondrogenic region of fish fins<sup>21</sup>. Despite these advances, however, little is known about the contribution of different

*hox* paralogues—individually and in combination—to the adult fin phenotype and the origin of cells that give rise to the distal fin skeleton. While previous studies have shown that osteoblasts of the fin rays in the caudal fin of zebrafish are derived from either neural crest or paraxial mesoderm, the source of osteoblasts in pectoral fin rays is currently unknown<sup>22–24</sup>. Consequently, it remains unclear where the cellular and genetic markers of the autopod of the tetrapod limb reside in fish fins.

In order to bridge these gaps in knowledge, we followed the fates of cells marked by early and late phase *hox* enhancers to adult stages in pectoral fins. In addition, we engineered zebrafish that completely lacked each individual *hox13* gene, and bred stable lines with multiple gene knockout combinations of *hox* paralogues. The power of these experiments is twofold: 1) to our knowledge, they represent the first functional analyses of *hox* activity in fins, and 2) they enable a direct developmental comparison to experiments performed in tetrapod limbs.

We performed *in situ* hybridization of *hoxa13a*, *hoxa13b*, and *hoxd13a* genes from 48–120 h post fertilization (hpf) in zebrafish to determine whether active *hox* expression has a role in the development of the pectoral fin fold. *Hoxa13* genes in zebrafish are expressed in the distal fin mesenchyme at 48 hpf and weakly in the proximal portion of the pectoral fin fold from 72–96 hpf, indicating that *hoxa13* genes are not actively expressed in the developing fold<sup>18</sup> (Fig. 1a, b). *Hoxd13a* is expressed in the posterior half of the fin, but it becomes weak after 96 hpf (Fig. 1c). *Hox* expression is entirely absent in fins 10 days post fertilization (dpf) (Extended Data Fig. 1). As *hox13* genes do not appear to have a main role in zebrafish fin fold development past 72–96 hpf, we sought to determine what structures *hox*-positive cells populate in the developing and adult folds.

To follow the fates of cells that experience early phase activity in the zebrafish fin, we modified our previously reported transgenesis vector<sup>21</sup> to express Cre-recombinase driven by the zebrafish early-phase enhancer CNS65<sup>25</sup>. This enhancer activates expression throughout the endochondral disk of pectoral fins from 31 to ~38 hpf (Fig. 2a and Extended Data Fig. 1). Stable lines expressing CNS65x3-Cre were crossed to the lineage-tracing zebrafish line Tg(*ubi:Switch*) fish, in which cells that express Cre are permanently labelled with mCherry<sup>26</sup>. At 6 dpf mesenchymal cells in which expression was driven by CNS65 at 38 hpf make up the entire endochondral disk of the pectoral fin (Fig. 2b). We also found mCherry-positive cells in the fin fold at 6 dpf and extensively at 20 dpf (Fig. 2b). These cells contained filamentous protrusions extending distally as well as nuclei positioned at the posterior side, both of which suggest that the cells were migrating distally out of the endochondral disk (Fig. 2b).

To determine the fate of late phase cellular activity, we employed the same fate-mapping strategy but used a late phase *hoxa* enhancer (e16) from the spotted gar (*Lepisosteus oculatus*) genome<sup>21</sup>. We chose a *hoxa* enhancer because lineage-tracing data in mouse has shown that late phase *Hoxa13* cells in the limb make up the osteoblasts of the wrist and digits exclusively, making it a *bona fide* marker of the autopod<sup>5</sup>.

<sup>1</sup>Department of Organismal Biology and Anatomy, University of Chicago, Chicago, Illinois 60637, USA.

\*These authors contributed equally to this work.

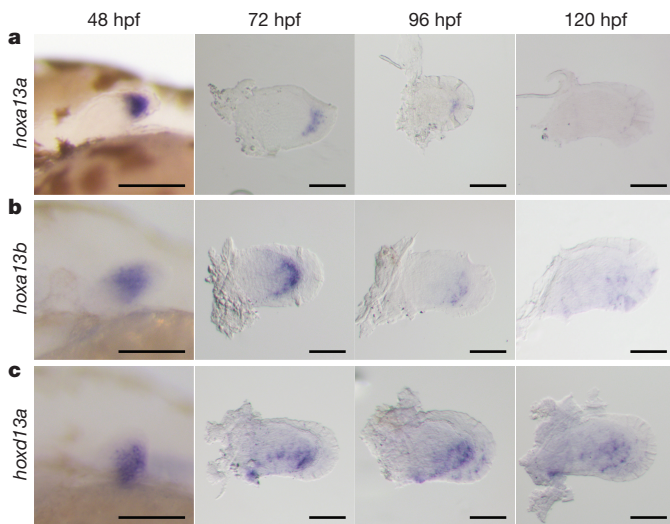


**Figure 1 | Expression patterns of *hoxa13* genes at 48–120 hpf.** **a**, *hoxa13a*. **b**, *hoxa13b*. **c**, *hoxd13a*. *Hoxa13a* is expressed in distal mesenchyme at 48 hpf, but expression continues in the proximal fin fold from 72 to 96 hpf (a). *Hoxa13b* is expressed in distal mesenchyme and expression can be observed at the distal part of the endochondral disk until 96 hpf (b). *Hoxd13a* is expressed in the posterior half of the mesenchyme at 48 hpf and expression continues in the posterior endochondral disk through 96 hpf. After 96 hpf, expression becomes weak (c). Scale bars are 100 µm.  $n = 20$  embryos for each *in situ* hybridization at 48 hpf.  $n = 10$  embryos after 72 hpf.

In addition, gar e16 (which has no sequence conservation in zebrafish) drives expression throughout the autopod in transgenic mice in a pattern that mimics the endogenous murine enhancer and *Hoxa13* expression<sup>21,27</sup>. In transgenic zebrafish, gar e16 is active in the distal portion of the endochondral disk of the pectoral fin at 48 hpf, and ceases activity after approximately 55 hpf (Fig. 2a and Extended Data Fig. 1). When these transgenic zebrafish were crossed to Tg(*ubi:Switch*), at 6 dpf we detected the majority of mCherry-positive cells in the developing fin fold with a small number of cells lining the distal edge of the endochondral disk (Fig. 2c). At 20 dpf, the fin fold contained nearly all of the mCherry-positive cells, which had formed tube-like cells that appeared to be developing actinotrichia (Fig. 2c). In adult fish (90 dpf), late phase cells were restricted to the adult structures of the fin fold, where they composed osteoblasts that make up the fin rays, among other tissues (Fig. 2d). As the e16 enhancer is active only in the distal endochondral disk at 48 hpf, and the labelled cells end up in the fin rays of the adult, late phase *hox*-positive cells are likely to migrate from the endochondral portion of the fin into the fin fold, a hypothesis supported by extensive filopodia in mCherry-positive cells projecting in the direction of the distal edge of the fin (Fig. 2c).

To explore the function of *hoxa13* genes, we inactivated individual *hoxa13* genes from the zebrafish genome by CRISPR/Cas9 and also made combinatorial deletions through genetic crosses of stable lines (Extended Data Fig. 2 and Extended Data Table 2, 3 and 4). Homozygous null embryos for individual *hoxa13* genes exhibited embryonic pectoral fins that were comparable in size with the wild type at 72 hpf (Extended Data Fig. 3). The shape and size of the fin fold and endochondral disk were also assayed by *in situ* hybridization for *and1* and *shha*, which serve as markers for the developing fin fold and endochondral disk, respectively<sup>28</sup> (Extended Data Fig. 3). In adult fins (~120 dpf), we observed no detectable difference in the length of fin rays of *hoxd13a*<sup>-/-</sup> mutants when compared to wild-type fish (Fig. 3d and Extended Data Fig. 4). However, both *hoxa13a*<sup>-/-</sup> and *hoxa13b*<sup>-/-</sup> single mutant fish retained fin rays that were shorter than the wild type, suggesting a role for *hoxa13* genes in fin ray development (Fig. 3g, j and Extended Data Fig. 4). To determine the degree to which endochondral bones were affected, we used CT scanning technology

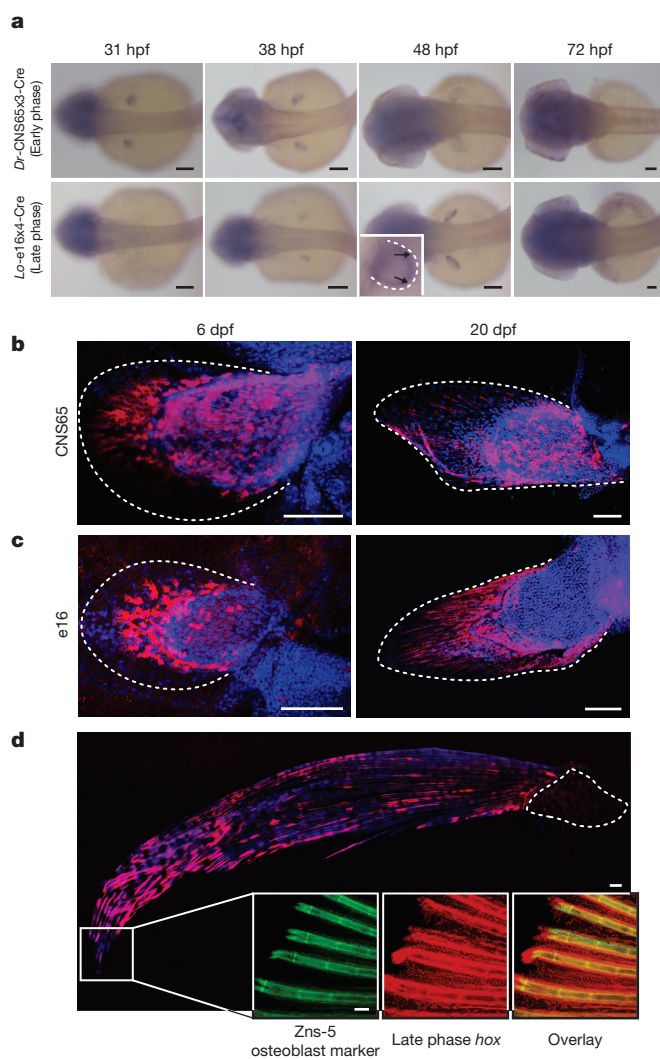


**Figure 2 | Fate mapping of cells marked by the activity of *hox* enhancers.** **a**, *In situ* hybridization of Cre in *Dr-CNS65x3-Cre* and *Lo-e16x4-Cre* exhibits expression dynamics of early and late phase enhancers used for fate mapping. Cre regulated by early phase *hox* enhancer CNS65 is expressed throughout the fin from 31 to 38 hpf, whereas late phase expression (driven by e16) begins weakly in the distal fin at 38 hpf and ceases at ~55 hpf. Inset shows zoom in of the pectoral fin, black arrows point to the distal border of the endochondral disk. **b**, Lineage tracing of *Dr-CNS65x3-Cre* at 6 dpf and 20 dpf. Red: mCherry IF; blue: DAPI. Cells that experienced early phase expression (red) contribute to fin fold and endochondral disk. **c**, Lineage tracing of *Lo-e16x4-Cre* at 6 dpf and 20 dpf. Cells that underwent late phase expression are present mostly in the fin fold, though some cells are at the distal edge of the disk. Red cells at 6 dpf protrude filopodia in the distal direction, indicating that these cells are actively moving out into the fin fold. **d**, Lineage tracing of late phase *hox* cells in adult zebrafish fin (~120 dpf). mCherry cells are present only in the derivatives of the fin fold, and not in the endochondral disk. Inset: magnification of distal edge of fin rays. Green: Zns-5 osteoblast marker; red: Hox-positive; yellow: overlap of Zns5 and Cre. White dotted lines outline the fin (**b**, **c**) or endochondral bones in (**d**).  $n = 5$  for stable lines. All scale bars are 100 µm except for the total fin in **d**, which is 500 µm.

for wild-type and mutant adult fish. Each single mutant, *hoxa13a*<sup>-/-</sup>, *a13b*<sup>-/-</sup> or *d13a*<sup>-/-</sup>, had four proximal radials and 6–8 distal radials with similar morphology to those of wild-type zebrafish (Fig. 3c, f, i, l and Extended Data Fig. 4). We crossed heterozygous mutants to obtain fish that lacked all *hoxa13* genes (*hoxa13a*<sup>-/-</sup>, *a13b*<sup>-/-</sup>). The fin folds of *hoxa13a*<sup>-/-</sup>, *a13b*<sup>-/-</sup> embryos were ~30% shorter than the wild type at 72 and 96 hpf, whereas the number of cells in the endochondral disk was ~10% greater (Extended Data Fig. 5). Adult

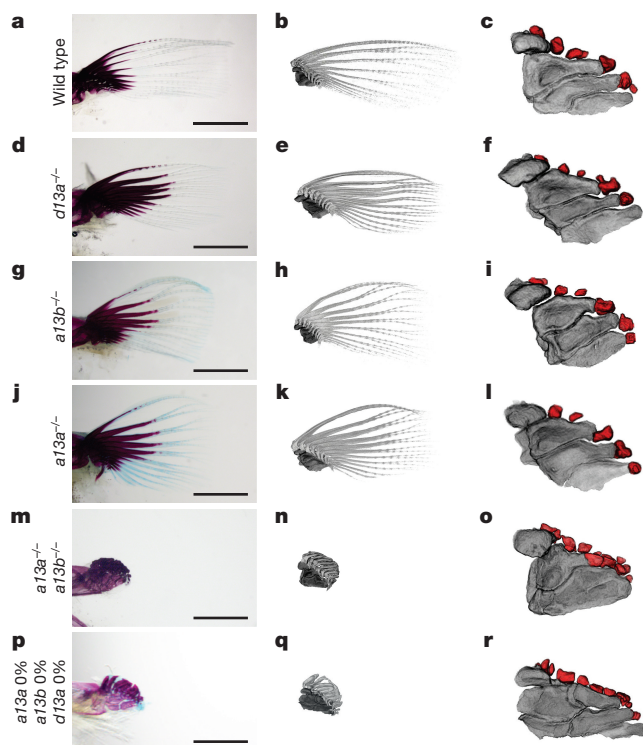


**Figure 3 | Adult fin phenotypes of *hox13* deletion series.** **a–c**, wild type. **d–f**, *hoxd13a*<sup>-/-</sup>. **g–i**, *hoxa13b*<sup>-/-</sup>. **j–l**, *hoxa13a*<sup>-/-</sup>. **m–o**, *hoxa13a*<sup>-/-</sup>, *a13b*<sup>-/-</sup>. **p–r**, *hoxa13a*0% *a13b*0% and *d13a*0% (mosaic triple knockout; Methods and Extended Data Tables 3, 4). Each mutant *hox* sequence is found in Extended Data Tables 3, 4. **a, d, g, j, m, p**, Alzarin Red and Alcian Blue staining of pectoral fin. **b, e, h, k, n, q**, CT scanning of pectoral fins. Black: radials (endochondral bones); grey: fin rays (dermal bones). Note that *hoxa13* single (**g, h, j, k**), double (**m, n**), and mosaic triple (**p, q**) mutant fins show shorter fin rays than wild type (**a, b**). Fins were scaled according to the bone staining pictures. **c, f, i, l, o, r**, Enlarged images of CT scanning without fin rays to reveal endochondral patterns. Dark grey: proximal radials; red: distal radials. Upper left side is the anterior and bottom right is the posterior side in each picture. Double and triple knockout mutants have 10–13 distal radials (**o** and **r**; Extended Data Fig. 4, Supplementary Information). Third and fourth proximal radials started to fuse into one bone in *hoxa13a*<sup>-/-</sup>, *a13b*<sup>-/-</sup> (**o**). Note that posterior distal radials are stacked along proximodistal axis (**o**). Posterior proximal radials are broken down into small parts in mosaic triple knockout (**r**). Scale bars are 2 mm. The size of specimens are not scaled in **c, f, i, l, o** and **r** to display the detail of distal radials. *n* = 3 fish for single and double mutants and *n* = 5 fish for mosaic triple mutant.

*hoxa13a*<sup>-/-</sup>, *a13b*<sup>-/-</sup> fish exhibited greatly reduced fin rays (Fig. 3m, Extended Data Fig. 4 and Supplementary Information). In contrast to dermal reduction, the endochondral distal radials of double mutants were significantly increased to 10–13 in number, often stacked along the proximodistal axis (Fig. 3o, Extended Data Fig. 4 and Supplementary Information,  $P=0.0014$ , *t*-test comparing the means). A similar pattern was seen in triple knockout fish (mosaic for *hoxa13b* and *hoxd13a*) (Fig. 3p–r and Extended Data Fig. 4) along with altered proximal radials, implying that late phase *hox* genes are involved in patterning the proximal endochondral radials of fins, unlike their role in tetrapods (Fig. 3).

Despite being composed of different kinds of skeletal tissue, fin rays and digits share a common population of distal mesenchymal cells that experience late phase *Hox* expression driven by shared regulatory architectures and enhancer activities<sup>21</sup>. In addition, loss of 5' *Hox* activity results in the deletion or reduction of both of these structures. Whereas phylogenetic evidence suggests that rays and digits are not homologous in terms of morphology, the cells and regulatory processes in both the fin fold and the autopod share a deep homology that may be common to both bony fish and jawed vertebrates<sup>19</sup>.

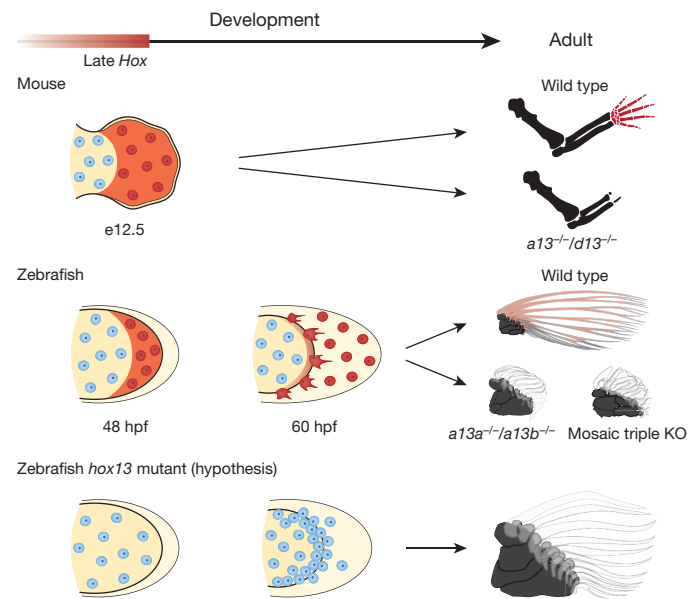


**Figure 4 | Shared developmental histories in fin rays and digits.** In mice (top row), late phase *Hox* expression (red) marks the distal cells of the limb bud that result in bones of the autopod (wrists and digits). Double knockout of *Hoxa13* and *Hoxd13* results in the loss of the autopod. In zebrafish wild-type fins (middle row), cells marked by late phase *hox* expression (red) end up in the fin fold and within osteoblasts of the dermal rays. *Hoxa13* double knockout fish (*hoxa13a*<sup>-/-</sup>, *a13b*<sup>-/-</sup>) and the triple knockout (mosaic for *hoxa13b* and *hoxd13a*) have extremely reduced fin rays with increased distal endochondral radials. Note that distal radials are stacked along the proximodistal axis in the posterior of the fins. The results lead to the hypothesis (bottom row) that the knockout phenotype results from a deficit in migration of mesenchymal cells with more cells left in the distal fin bud (increased number of cells in the endochondral disk of mutants fins, Extended Data Fig. 4) and fewer migrating to the fold, thereby resulting in a larger number of endochondral bones and reduced dermal ones. Red cells: cells that experienced late phase *hox* expression. Mouse limbs consist of only endochondral (black) and dermal (transparent; fin rays) bones.

Two major trends underlie the fin-to-limb transition—the elaboration of endochondral bones and the progressive loss of the extensive dermal fin skeleton<sup>2,7,20</sup>. In the combinatorial knockouts of *hox13* genes, which in tetrapods result in a loss of the autopod, distal endochondral radials were increased in number while fin rays were greatly reduced. As a common population of cells in the distal appendage is involved in the formation of rays and digits, the endochondral expansion in tetrapod origins may have occurred through the transition of distal cellular fates and differential allocation of cells from the fin fold to the fin bud<sup>18</sup> (Fig. 4). The two major trends of skeletal evolution in the fin-to-limb transition may be linked at cellular and genetic levels.

**Online Content** Methods, along with any additional Extended Data display items and Source Data, are available in the online version of the paper; references unique to these sections appear only in the online paper.

Received 7 April; accepted 20 July 2016.

Published online 17 August 2016.

- Clack, J. A. *Gaining Ground: The Origin and Evolution of Tetrapods*. Indiana University Press, Indiana (2012).
- Clack, J. A. The fin to limb transition: New data, interpretations, and hypotheses from paleontology and developmental biology. *Annu. Rev. Earth Planet. Sci.* **37**, 163–179 (2009).
- Schneider, I. & Shubin, N. H. The origin of the tetrapod limb: from expeditions to enhancers. *Trends Genet.* **29**, 419–426 (2013).
- Fromental-Ramain, C. et al. *Hoxa-13* and *Hoxd-13* play a crucial role in the patterning of the limb autopod. *Development* **122**, 2997–3011 (1996).
- Scotti, M., Kherdjemil, Y., Roux, M. & Kmita, M. A *Hoxa13*:Cre mouse strain for conditional gene manipulation in developing limb, hindgut, and urogenital system. *Genesis* **53**, 366–376 (2015).

6. Grandel, H. & Schulte-Merker, S. The development of the paired fins in the zebrafish (*Danio rerio*). *Mech. Dev.* **79**, 99–120 (1998).
7. Coates, M. I., Ruta, M. & Friedman, M. Ever since Owen: Changing perspectives on the early evolution of tetrapods. *Annu. Rev. Ecol. Evol. Syst.* **39**, 571–592 (2008).
8. Thorogood, P. *The Development of the Teleost Fin and Implications for Our Understanding of Tetrapod Limb Evolution*. (Springer US, 1991).
9. Fernandez-Teran, M. & Ros, M. A. The apical ectodermal ridge: morphological aspects and signaling pathways. *Int. J. Dev. Biol.* **52**, 857–871 (2008).
10. Zeller, R., López-Ríos, J. & Zuniga, A. Vertebrate limb bud development: moving towards integrative analysis of organogenesis. *Nat. Rev. Genet.* **10**, 845–858 (2009).
11. Yano, T., Abe, G., Yokoyama, H., Kawakami, K. & Tamura, K. Mechanism of pectoral fin outgrowth in zebrafish development. *Development* **139**, 2916–2925 (2012).
12. Sordino, P., van der Hoeven, F. & Duboule, D. Hox gene expression in teleost fins and the origin of vertebrate digits. *Nature* **375**, 678–681 (1995).
13. Woltering, J. M. & Duboule, D. The origin of digits: expression patterns versus regulatory mechanisms. *Dev. Cell* **18**, 526–532 (2010).
14. Gehrke, A. R. & Shubin, N. H. Cis-regulatory programs in the development and evolution of vertebrate paired appendages. *Semin. Cell Dev. Biol.* <http://dx.doi.org/10.1016/j.semcd.2016.01.015> (2016).
15. Zakany, J. & Duboule, D. The role of Hox genes during vertebrate limb development. *Curr. Opin. Genet. Dev.* **17**, 359–366 (2007).
16. Freitas, R., Zhang, G. & Cohn, M. J. Biphasic Hoxd gene expression in shark paired fins reveals an ancient origin of the distal limb domain. *PLoS One* **2**, e754 (2007).
17. Davis, M. C., Dahn, R. D. & Shubin, N. H. An autopodial-like pattern of Hox expression in the fins of a basal actinopterygian fish. *Nature* **447**, 473–476 (2007).
18. Ahn, D. & Ho, R. K. Tri-phasic expression of posterior Hox genes during development of pectoral fins in zebrafish: implications for the evolution of vertebrate paired appendages. *Dev. Biol.* **322**, 220–233 (2008).
19. Tulenko, F. J. et al. HoxD expression in the fin-fold compartment of basal gnathostomes and implications for paired appendage evolution. *Sci. Rep.* **6**, 22720 (2016).
20. Freitas, R., Gómez-Marín, C., Wilson, J. M., Casares, F. & Gómez-Skarmeta, J. L. HoxD13 contribution to the evolution of vertebrate appendages. *Dev. Cell* **23**, 1219–1229 (2012).
21. Gehrke, A. R. et al. Deep conservation of wrist and digit enhancers in fish. *Proc. Natl Acad. Sci. USA* **112**, 803–808 (2015).
22. Lee, R. T. H., Knapik, E. W., Thiery, J. P. & Carney, T. J. An exclusively mesodermal origin of fin mesenchyme demonstrates that zebrafish trunk neural crest does not generate ectomesenchyme. *Development* **140**, 2923–2932 (2013).
23. Lee, R. T. H., Thiery, J. P. & Carney, T. J. Dermal fin rays and scales derive from mesoderm, not neural crest. *Curr. Biol.* **23**, R336–R337 (2013).
24. Smith, M., Hickman, A., Amanze, D., Lumsden, A. & Thorogood, P. Trunk neural crest origin of caudal fin mesenchyme in the zebrafish *Brachydanio rerio*. *Proc. R. Soc. Lond. B* **256**, 137–145 (1994).
25. Braasch, I. et al. The spotted gar genome illuminates vertebrate evolution and facilitates human-teleost comparisons. *Nat. Genet.* **48**, 427–437 (2016).
26. Mosimann, C. et al. Ubiquitous transgene expression and Cre-based recombination driven by the ubiquitin promoter in zebrafish. *Development* **138**, 169–177 (2011).
27. Berlivet, S. et al. Clustering of tissue-specific sub-TADs accompanies the regulation of HoxA genes in developing limbs. *PLoS Genet.* **9**, e1004018 (2013).
28. Zhang, J. et al. Loss of fish actinotrichia proteins and the fin-to-limb transition. *Nature* **466**, 234–237 (2010).

**Supplementary Information** is available in the online version of the paper.

**Acknowledgements** We thank J. Westlund for figure preparation and construction, as well as maintenance of zebrafish facilities. M. Coates, M. Davis, R. Ho, I. Ruvinsky, J.-L. Gomez Skarmeta, and C. Tabin provided comments and advice. We thank L. I. Zon, C. Mosimann, and C. Lawrence for *Tg(ubi:Switch)* fish, M. L. Suster for the *pCR8GW-Cre-pA-FRT-kan-FRT* plasmid, R. Ho and S. Briscoe for insights regarding lineage-tracing experiments, V. Bindokas and the University of Chicago Integrated Light Microscopy Core Facility for assistance with imaging, L. Zhixi for use of the high-energy CT scanning facility of University of Chicago, M. E. Horb and M. C. Salanga of the National Xenopus Resource (RRID:SCR-013731) of the Marine Biological Laboratories for tutelage in applying CRISPR/Cas9, J. Gitlin, A. Latimer and R. Thomason for providing space for zebrafish CRISPR/Cas9 experiments and also maintaining juveniles, and the Marine Resource Center of the Marine Biological Laboratories for assistance with the transfer of mutant zebrafish between University of Chicago and the MBL. This study was supported by the Uehara Memorial Foundation Research Fellowship 2013, Japan Society for the Promotion of Science Postdoctoral Research Fellowship 2012-127, and Marine Biological Laboratory Research Award 2014 (to T.N.); National Institutes of Health Grant T32 HD055164 and National Science Foundation Doctoral Dissertation Improvement Grant 1311436 (to A.R.G.); and the Brinson Foundation and the University of Chicago Biological Sciences Division (to N.H.S.).

**Author Contributions** T.N., A.R.G. and N.H.S. designed research; T.N. and J.S. performed *in situ* hybridization and CRISPR experiments; A.R.G. did fate mapping of the *hox* enhancers; T.N. and J.L. obtained CT scanning data; T.N., A.R.G., J.L. and N.H.S. analyzed data; and T.N., A.R.G., J.L. and N.H.S. wrote the paper.

**Author Information** Reprints and permissions information is available at [www.nature.com/reprints](http://www.nature.com/reprints). The authors declare no competing financial interests. Readers are welcome to comment on the online version of the paper. Correspondence and requests for materials should be addressed to N.H.S. (nshubin@uchicago.edu).

**Reviewer Information** *Nature* thanks S. Burgess and the other anonymous reviewer(s) for their contribution to the peer review of this work.

## METHODS

All zebrafish work was performed according to standard protocols approved by The University of Chicago (ACUP #72074). No statistical methods were used to predetermine sample size. The experiments were not randomized and the investigators were not blinded to allocation during experiments and outcome assessment. **Whole-mount *in situ* hybridization.** *In situ* hybridization for the *hox13*, *Cre*, and *and1* and *shha* genes were performed according to standard protocols<sup>29</sup> after fixation in 4% paraformaldehyde overnight at 4 °C. Probes for *hox13* and *shha* were as previously described<sup>18</sup>. Primers to clone *Cre* and *and1* into vectors can be found in Extended Data Tables 1 and 2. Specimens were visualized on a Leica M205FA microscope.

**Lineage tracing vector construction.** In order to create a destination vector for lineage tracing, we first designed a random sequence of 298 bp that contained a SmaI site to be used in downstream cloning. This sequence was ordered as a gBlocks fragment (IDT) and ligated into the pCR8/GW/TOPO TA cloning vector (Invitrogen). We then performed a Gateway LR reaction according to the manufacturers specifications between this entry vector and pXIG-cFos-GFP, which abolished an NcoI site present in the gateway cassette and introduced a SmaI site. We then removed the GFP gene with NcoI and BglII of the destination vector and ligated in *Cre* with (primers in Extended Data Table 1), using the 'pCR8/GW-Cre-pA-FRT-kan-FRT' (kind gift of M. L. Suster, Sars International Center for Marine Molecular Biology, University of Bergen, Bergen, Norway) as a template for *Cre* PCR and Platinum Taq DNA polymerase High Fidelity (Invitrogen). In order to add a late phase enhancer to this vector, we first ordered four identical oligos (IDT gBlocks) of the core e16 sequence from gar, each flanked by different restriction sites. Each oligo was then ligated into pCR8/GW/TOPO, and sequentially cloned via restriction sites into a single pCR8/GW/TOPO vector. This entry vector was used a template to PCR the final *Lo-e16x4* sequence and ligate it into the *Cre* destination vector using XbaI and SmaI, creating *Lo-e16x4-Cre*. The early phase enhancer *Dr-CNS65x3* was cloned into the destination vector using the same strategy. Final vectors were confirmed by sequencing. A full list of sequences and primers used can be found in Extended Data Table 1.

**Establishment of lineage tracing lines.** \*AB zebrafish embryos were collected from natural spawning and injected according to the Tol2 system as described previously<sup>21</sup>. Transposase RNA was synthesized from the pCS2-zT2TP vector using the mMessage mMachine SP6 kit (Ambion)<sup>21</sup>. All injected embryos were raised to sexual maturity according to standard protocols. Adult F0 fish were outcrossed to wild-type \*AB, and the total F1 clutch was lysed and DNA isolated at 24 hpf for genotyping (see Extended Data Table 1 for primers) to confirm germline transmission of *Cre* plasmids in the F0 founders. Multiple founders were identified and tested for the strongest and most consistent expression via antibody staining and *in situ* hybridization. One founder fish was identified as best, and all subsequent experiments were performed using offspring of this individual fish.

**Lineage tracing crossing and detection.** Founder *Lo-e16x4-Cre* and *Dr-CNS65x3-Cre* fish were crossed to the Tg(*ubi:Switch*) line (kind gift from L. I. Zon). Briefly, this line contains a construct in which a constitutively active promoter (*ubiquitin*) drives expression of a loxP flanked GFP protein in all cells of the fish assayed. When *Cre* is introduced, the GFP gene is removed and the ubiquitin promoter is exposed to mCherry, thus permanently labelling the cell. We crossed our founder *Cre* fish to Tg(*ubi:Switch*) and fixed progeny at different time points to track cell fate. In order to detect the mCherry signal, embryos or adults were fixed overnight in 4% paraformaldehyde and subsequently processed for whole-mount antibody staining according to standard protocols<sup>30</sup> using the following antibodies and dilutions: 1st rabbit anti-mCherry/DsRed (Clontech #632496) at 1:250, 1st mouse anti-Zns-5 (Zebrafish International Resource Center, USA) at 1:200, 2nd goat anti-rabbit Alexa Fluor 546 (Invitrogen #A11071) at 1:400, 2nd goat anti-mouse Alexa 647 (Invitrogen #A21235) at 1:400. Stained zebrafish were mounted under a glass slide and visualized using an LSM 710 confocal microscope (Organismal Biology and Anatomy, the University of Chicago). Antibody stains on adult zebrafish (90 dpf) fins were imaged on a Leica SP5 II tandem scanner AOBS Laser Scanning Confocal (the University of Chicago Integrated Light Microscopy Core Facility).

**CRISPR/Cas9 design and synthesis.** Two mutations were simultaneously introduced into the first exon of each *hox13* gene by CRISPR/Cas9 system as previously described in *Xenopus tropicalis*<sup>31</sup>. Briefly, two gRNAs that match the sequence of exon 1 of each *hox13* gene were designed by ZiFiT (<http://zifit.partners.org/ZiFiT/>). To synthesize gRNAs, forward and reverse oligonucleotides that are unique for individual target sequences were synthesized by Integrated DNA Technologies, Inc. (IDT). Each oligonucleotide sequence can be found in Extended Data Table 2. Subsequently, each forward and reverse oligonucleotide were hybridized, and double stranded products were individually amplified by PCR with primers that include a T7 RNA promoter sequence, followed by purification by NucleoSpin Gel and PCR Clean-up Kit (Macherey-Nagel). Each gRNA was synthesized

from the purified PCR products by *in vitro* transcription with the MEGAscript T7 Transcription kit (Ambion). *Cas9* mRNA was synthesized by mMESSAGE mMACHINE SP6 Transcription Kit according to the manufacturer's instructions (Ambion).

**CRISPR/Cas9 injection and mutants selection.** Two gRNAs targeting exon 1 of each *hox* gene were injected with *Cas9* mRNA into zebrafish eggs at the one-cell stage. We injected ~2 nl of the injection solution (5 µl solution containing 1,000 ng of each gRNA and 500 ng *Cas9* diluted in nuclease-free water) into the single cell of the embryo. Injected embryos were raised to adulthood, and at three months were genotyped by extracting DNA from tail clips. Briefly, zebrafish were anaesthetized by Tricaine (0.004%) and tips of the tail fin (2–3 mm<sup>2</sup>) were removed and placed in an Eppendorf tube. The tissue was lysed in standard lysis buffer (10 mM Tris pH 8.2, 10 mM EDTA, 200 mM NaCl, 0.5% SDS, 200 µg/ml proteinase K) and DNA recovered by ethanol precipitation. Approximately 800–1,100 bp of exon 1 from each gene was amplified by PCR using the primers described in Extended Data Table 2. To determine whether mutations were present, PCR products were subjected to T7E1 (T7 endonuclease1) assay as previously reported<sup>32</sup>. After identification of mutant fish by T7E1 assay, detailed analysis of mutation patterns were performed by sequencing at the Genomics Core at the University of Chicago.

**Establishment of *hox13* single and double mutant fish.** Identified mutant fish were outcrossed to wild type to select frameshift mutations from mosaic mutational patterns and establish single heterozygous lines. Obtained embryos were raised to adults (~3 months), then analysed by T7E1 assay and sequenced. Among a variety of mutational patterns, fish that have frameshift mutations were used for assays as single heterozygous fish. We obtained several independent heterozygous mutant lines for each *hox13* gene to compare the phenotype among different frameshift mutations. To obtain *hoxa13a*<sup>+/−</sup>, *hoxa13b*<sup>+/−</sup> double heterozygous mutant fish, each single heterozygous mutant line was crossed with the other mutant line. Offspring were analysed by T7E1 assay and sequenced after three months, and double heterozygous mutant fish were selected. To generate double homozygous *hoxa13* mutant embryos and adult fish (*hoxa13a*<sup>−/−</sup>, *hoxa13b*<sup>−/−</sup>), double heterozygous fish (*hoxa13a*<sup>+/−</sup>, *hoxa13b*<sup>+/−</sup>) were crossed with each other. The ratio of each genotype from crossing heterozygous fish is summarized in Extended Data Table 4.

**Genotype of single (*hoxa13a*<sup>−/−</sup> or *hoxa13b*<sup>−/−</sup>) or double (*hoxa13a*<sup>−/−</sup>, *hoxa13b*<sup>−/−</sup>) mutant by PCR.** After mutant lines were established, single (*hoxa13a* or *hoxa13b*) or double (*hoxa13a*, *hoxa13b*) mutant embryos and adult fish were genotyped by PCR for each analysis. Primer sequences for PCR are listed in Extended Data Table 2. To identify an 8 bp deletion in exon 1 of *hoxa13a*, the PCR product was treated by AvaI at 37 °C for 2 h, because the 8 bp deletion produces a new AvaI site in the PCR product ('zebra *hoxa13a*\_8\_bp del' primers, wild type; 231 bp, mutant; 111 bp and 119 bp). Final product size was confirmed by 3% agarose gel electrophoresis. To identify a 29 bp deletion in exon 1 of *hoxa13a*, the PCR product was confirmed by gel electrophoresis ('zebra *hoxa13a*\_29\_bp del' primers, wild type; 110 bp, mutant; 81 bp). To identify a 14 bp insertion in exon 1 of *hoxa13b*, the PCR product was treated by Bcc1 at 37 °C for 2 h, because the 14 bp insertion produces a new Bcc1 site in the PCR product ('zebra *hoxa13b*\_14\_bp ins' primers, wild type; 98 bp, mutant; 53 bp + 57 bp). The final product size was confirmed by 3% agarose gel electrophoresis. The details of the mutant sequence are summarized in Extended Data Table 3a–c.

**Combination of stable and transient deletion of all *hox13* genes by CRISPR / Cas9.** Two gRNAs targeting exon 1 of *hoxa13b* and two gRNAs targeting exon 1 of *hoxd13a* were injected with *Cas9* mRNA into zebrafish one-cell eggs that were obtained from crossing *hoxa13a*<sup>+/−</sup> and *hoxa13a*<sup>+/−</sup>, *hoxa13b*<sup>+/−</sup>, *hoxd13a*<sup>+/−</sup> (gRNAs were same as that were used to establish single *hox13* knockout fishes and found in Extended Data Table 2). Injected eggs were raised to adult fish and genotyped by extracting DNA from tail fins. PCR products of each *hox13* gene were cloned into PCRIITOPO (Invitrogen) and deep sequencing was performed (Genomic Core, the University of Chicago). At four months old, skeletal staining and CT scanning were performed to analyse the effect of triple gene deletions. The knockout ratios of each *hox13* allele were calculated from the results of deep sequencing.

**Measurement of the fin fold length.** Embryos were obtained by crossing *hoxa13a*<sup>+/−</sup>, *hoxa13b*<sup>+/−</sup> to each other and raised to 72 hpf or 96 hpf. After fixation by 4% PFA for 15 h, caudal halves were used for PCR genotyping. Pectoral fins of wild type and *hoxa13a*<sup>−/−</sup>, *hoxa13b*<sup>−/−</sup> were detached from the embryonic body and placed horizontally on glass slides. The fins were photographed with a Leica M205FA microscope, and the fin fold length along the proximodistal axis at the centre of the fin was measured using ImageJ. The resulting data were analysed by t-test comparing the means.

**Counting the cell number in endochondral disk.** Embryos were obtained by crossing *hoxa13a*<sup>+/−</sup>, *hoxa13b*<sup>+/−</sup> to each other and raised to 96 hpf. After fixation by 4% PFA for 15 h, caudal halves were used for PCR genotyping. Wild type

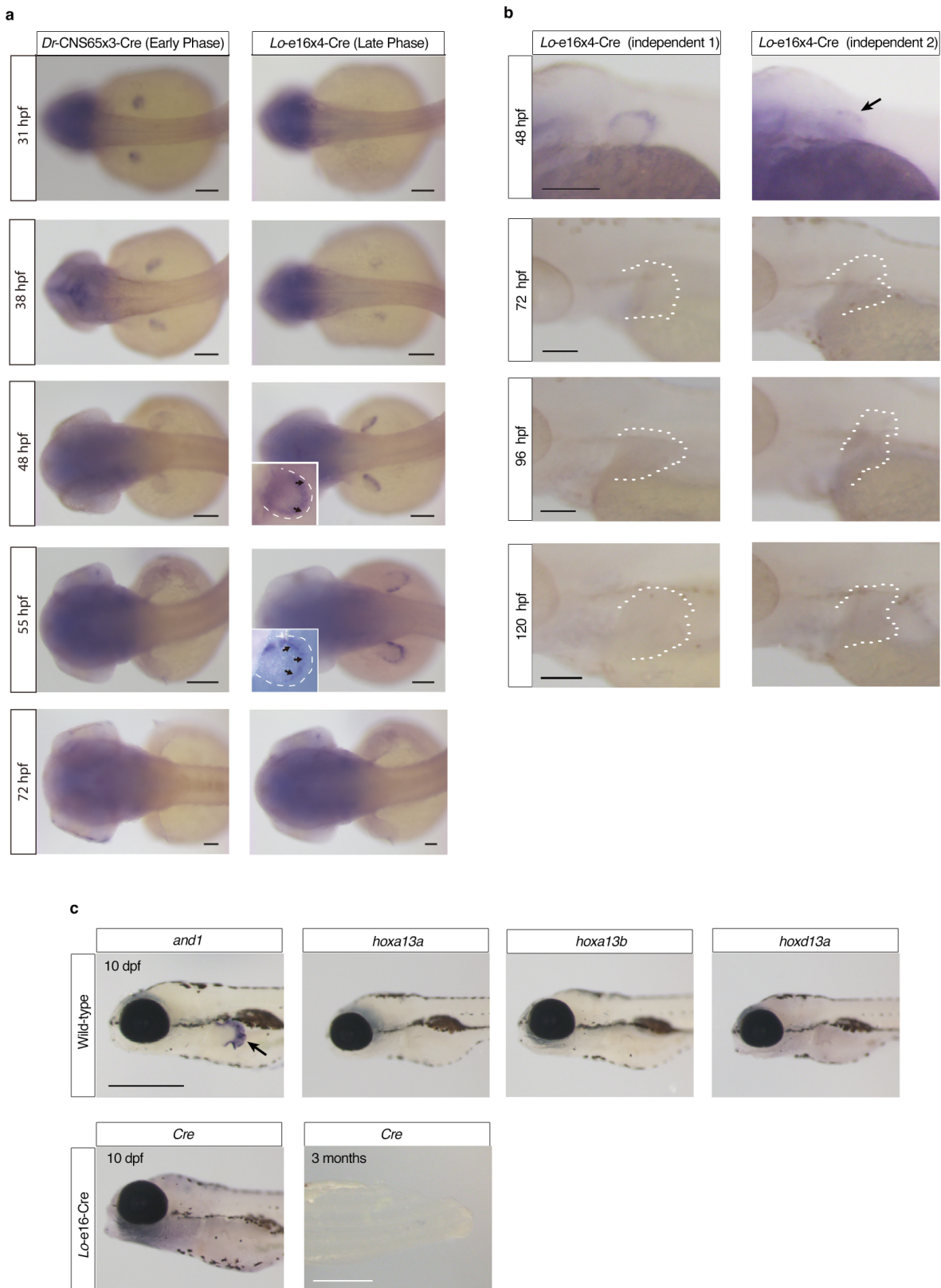
and *hoxa13a*<sup>-/-</sup>, *hoxa13b*<sup>-/-</sup> embryos were stained by DAPI (1:4,000 in PBS–0.1% Triton) for 3 h and washed for 3 h by PBS–0.1% Triton. Pectoral fins were detached from the embryonic body, placed on glass slides and covered by a coverslip. The DAPI signal was detected by Zeiss LSM 710 (Organismal Biology and Anatomy, the University of Chicago). Individual nuclei were manually marked using Adobe Illustrator and the number of nuclei was counted. The data were analysed by *t*-test comparing the means.

**Adult fish skeletal staining.** Skeletal staining was performed as previously described<sup>33</sup>. Briefly, fish were fixed in 10% neutral-buffered formalin overnight. After washing with milli-Q water, solutions were substituted by 70% EtOH in a stepwise fashion and then by 30% acetic acid/70% EtOH. Cartilage was stained with 0.02% alcian blue in 30% acetic acid/70% EtOH overnight. After washing with milli-Q water, the solution was changed to a 30% saturated sodium borate solution and incubated overnight. Subsequently, specimens were immersed in 1% trypsin/30% saturated sodium borate and incubated at room temperature overnight. Following a milli-Q water wash, specimens were transferred into a 1% KOH solution containing 0.005% Alzarin Red S. The next day, specimens were washed with milli-Q water and subjected to glycerol substitution. Three replicates for each genotype were investigated.

**PMA staining and CT scanning.** After skeletal staining, girdles and pectoral fins were manually separated from the body. Girdles and fins were stained with 0.5%

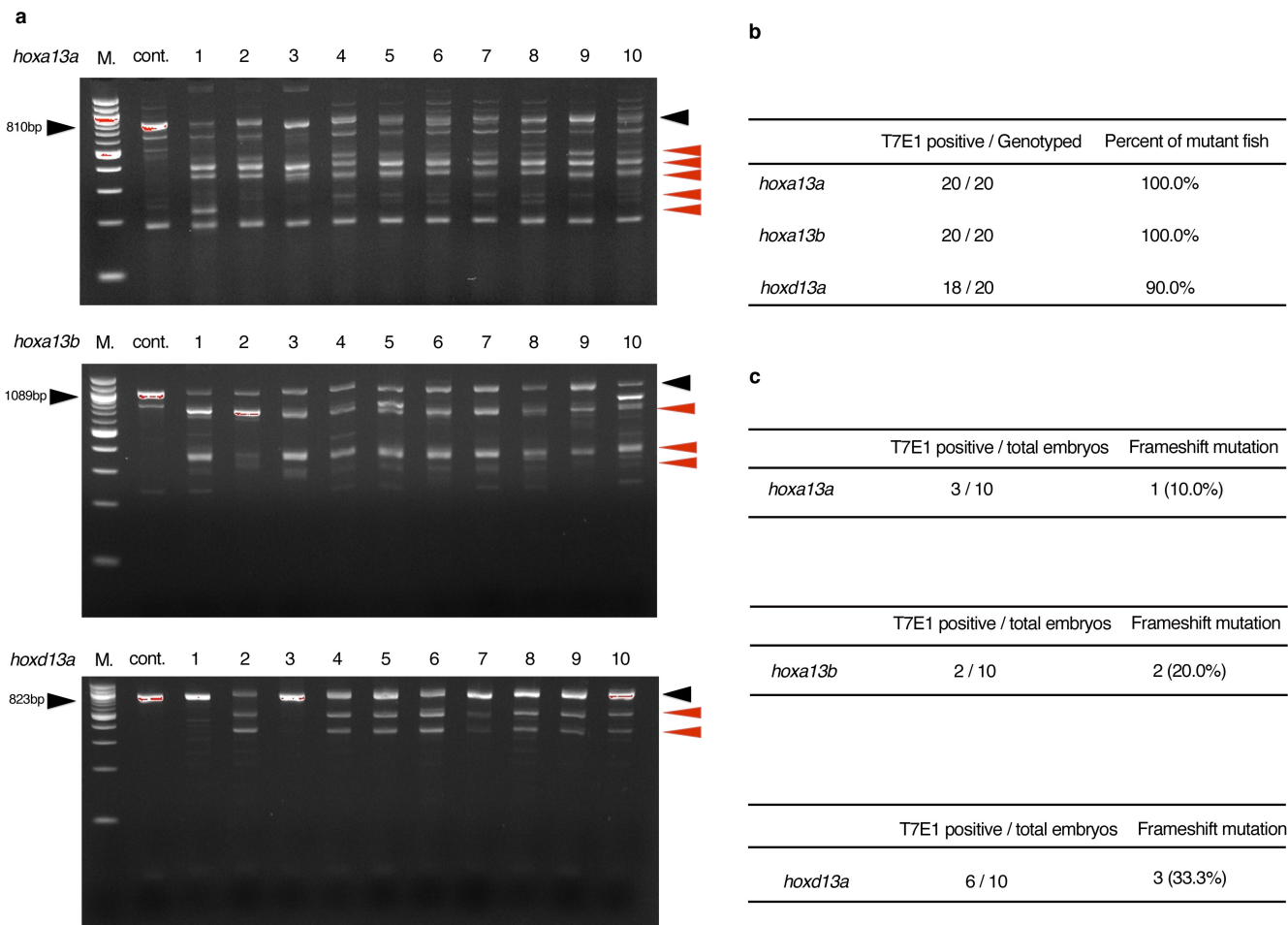
PMA (phosphomolybdic acid) in milli-Q water for 16 h and followed by washes with milli-Q water. Specimens were placed into 1.5 ml Eppendorf tubes with water and kept overnight to settle in the tubes. The next day, tubes containing specimens were set and scanned with the UChicago PaleoCT scanner (GE Phoenix v/tome/x 240kv/180kv scanner) (<http://luo-lab.uchicago.edu/paleoCT.html>), at 50 kVp, 160 µA, no filtration, 5×-averaging, exposure timing of 500 ms per image, and a resolution of 8 µm per slice (512 µm<sup>3</sup> per voxel). Scanned images were analysed and segmented using Amira 3D Software 6.0 (FEI). Three replicates for single and double homozygotes and five for mosaic triple knockout were investigated.

29. Thisse, C., Thisse, B. & Postlethwait, J. H. Expression of snail2, a second member of the zebrafish snail family, in cephalic mesendoderm and presumptive neural crest of wild-type and spadetail mutant embryos. *Dev. Biol.* **172**, 86–99 (1995).
30. Asharani, P. V. et al. Attenuated BMP1 function compromises osteogenesis, leading to bone fragility in humans and zebrafish. *Am. J. Hum. Genet.* **90**, 661–674 (2012).
31. Nakayama, T. et al. Simple and efficient CRISPR/Cas9-mediated targeted mutagenesis in *Xenopus tropicalis*. *Genesis* **51**, 835–843 (2013).
32. Jao, L.-E., Wente, S. R. & Chen, W. Efficient multiplex biallelic zebrafish genome editing using a CRISPR nuclease system. *Proc. Natl Acad. Sci. USA* **110**, 13904–13909 (2013).
33. Westerfield, M. *ZFIN: Zebrafish Book*. 4th ed. (Univ. of Oregon Press, 2000).



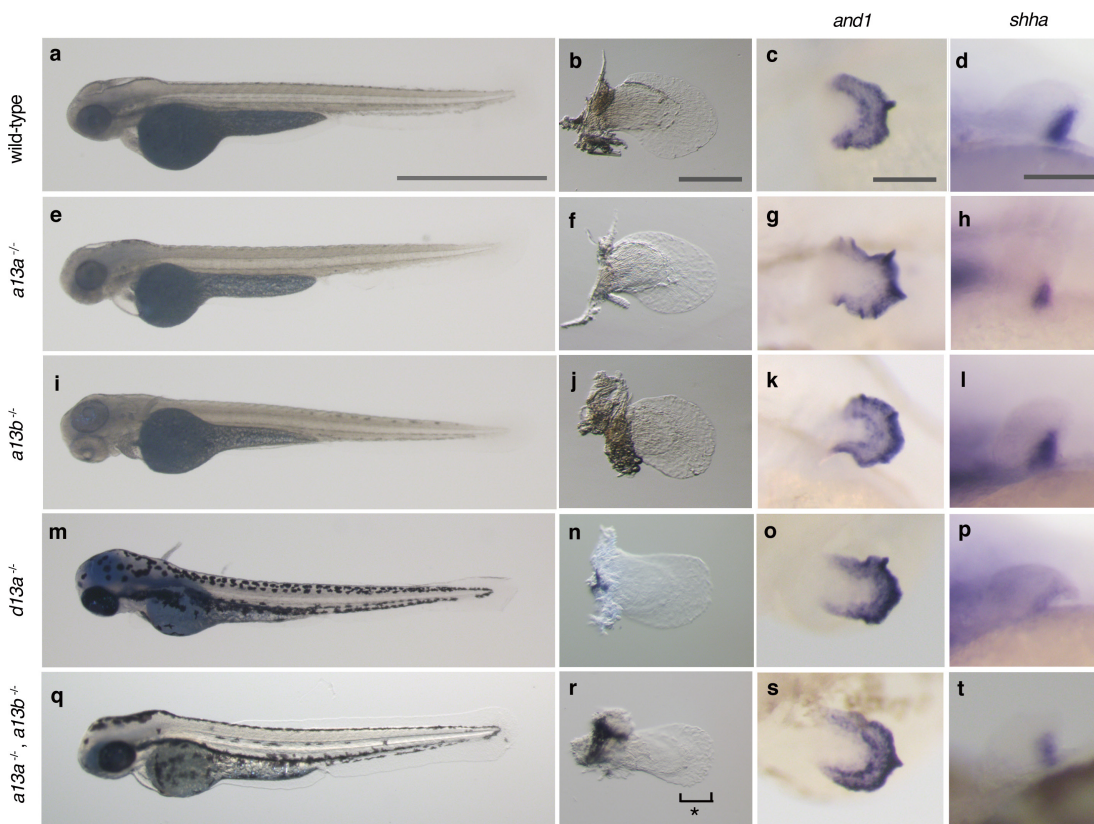
**Extended Data Figure 1 | Cre *in situ* hybridization of lineage tracing fish.** **a**, Cre is expressed only from 31 hpf to 38 hpf in *Dr-CNS65x3-Cre*, whereas it is expressed from 38 hpf to 55 hpf in *Lo-e16x4-Cre*. These temporal expression patterns of Cre indicate that our transgenic lineage tracing labelled the cells which experienced only early or late phase *hox*. Scale bars are 100 µm. **b**, Cre expression pattern from 48–120 hpf in independent *Lo-e16x4-Cre* lines (different founders from a). The fin is outlined by a dashed white line. The expression patterns from different founders were investigated and all expression ceases before 72 hpf. Our *in situ* results indicate that *Lo-e16x4-Cre* marks only the cells that

experienced late phase *hox* expression from 38–55 hpf.  $n = 5$  embryos for all stages. Scale bars are 100 µm. **c**, The expression pattern of *and1* and *hox13* genes in wild type (10 dpf) and also Cre in *Lo-e16x4-Cre* line (10 dpf and 3 months,  $n = 10$ ). Whereas *and1* expression can be observed in fin fold (positive control, black arrow), *hox13* genes are not expressed at 10 dpf in the wild type. Cre is not expressed at 10 dpf and at 3 months in the fin, indicating that *Lo-e16x4-Cre* activity is limited to only early embryonic development (38–55 hpf). Three month fins were dissected from the body of *Lo-e16x4-Cre* lines and subjected to *in situ* hybridization ( $n = 3$ ). Scale bars are 500 µm at 10 dpf and 3 months.



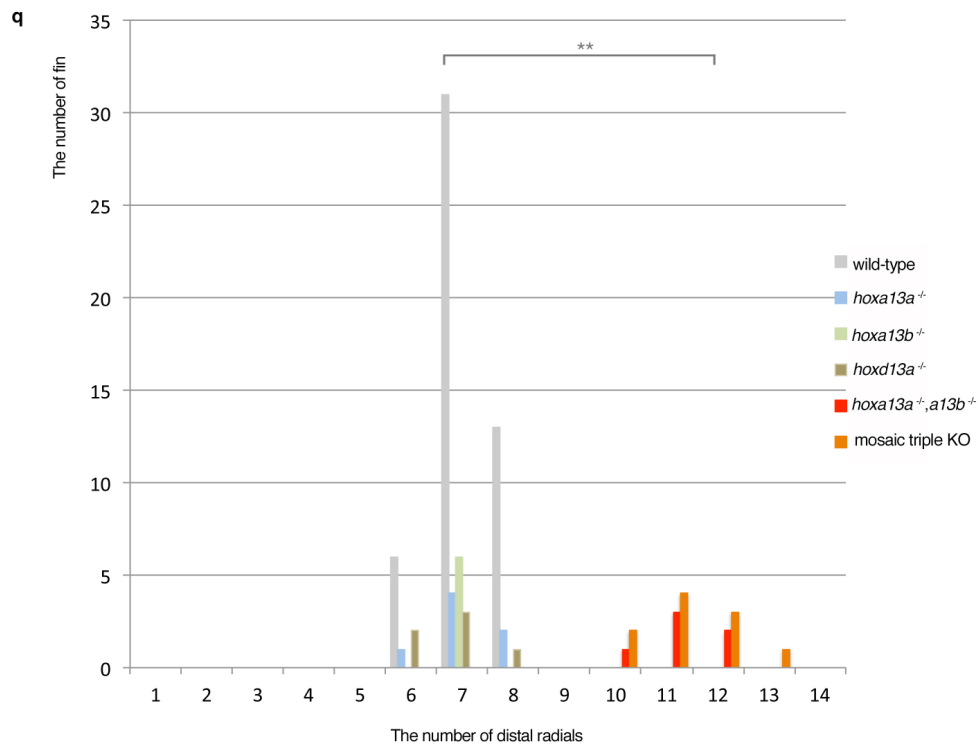
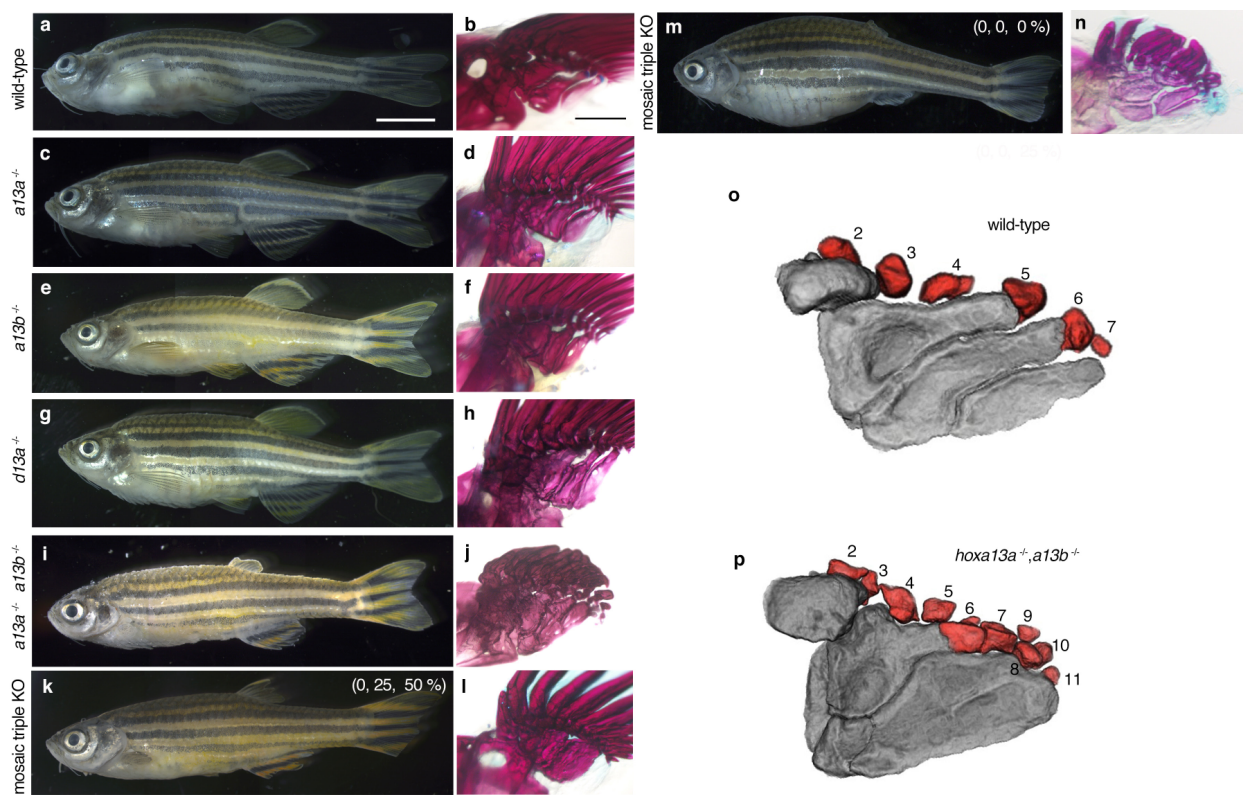
**Extended Data Figure 2 | T7E1 assay of F0 CRISPR/Cas9 adult fish.** PCR products of *hoxa13a*, *hoxa13b* or *hoxd13a* were subjected to a T7E1 assay (Methods) and confirmed by gel electrophoresis. **a**, The result of the *hoxa13a*, *hoxa13b* or *hoxd13a* T7E1 assay for ten adult fish. ‘M’ is a 100 bp DNA ladder marker (NEB). In the *hoxa13a* gel picture, 810 bp (black arrowhead) is the wild-type band as observed in cont. lane (wild type without gRNA injection). All ten fish showed smaller and bottom shifted products (red arrowheads) compared to negative control fish, indicating that all fish have mutations in the target region of *hoxa13a*. In the *hoxa13b* gel picture, 1,089 bp is the wild-type band. All ten fish into which *hoxa13b* gRNAs were injected showed smaller and bottom shifted products compared to negative control fish, indicating that all fish have

mutations in the target region of *hoxa13b*. In the *hoxd13a* gel picture, 823 bp is the wild-type band. Eight of ten fish showed smaller and bottom shifted products, indicating that 80% of fish have mutations in the target region of *hoxd13a*. **b**, The efficiency of CRISPR/Cas9 deletion for *hox13* in zebrafish. Almost all adult fish into which gRNAs and Cas9 mRNA were injected have mutations at the target positions. **c**, The efficiency of germline transmission of CRISPR/Cas9 mutant fish. Identified mutant fish were outcrossed to wild-type fish to obtain embryos and confirmed germline transmission. Obtained embryos were lysed individually at 48 hpf, genotyped by T7E1 assay and sequenced. Because of CRISPR/Cas9 mosaicism, some different mutation patterns, which result in a non-frameshift or frameshift mutation, were observed.



**Extended Data Figure 3 | Embryonic phenotypes of *hox13* deletion mutants.** **a, e, i, m, q.** Whole body pictures at 72 hpf. **a**, Wild type, **e**, *hoxa13a*<sup>-/-</sup> (4 bp del./4 bp del.), **i**, *hoxa13b*<sup>-/-</sup> (4 bp del./14 bp ins.), **m**, *hoxd13a*<sup>-/-</sup> (5 bp ins./17 bp del.), and **q**, *hoxa13a*<sup>-/-</sup>, *hoxa13b*<sup>-/-</sup> double homozygous embryo (8 bp del./29 bp del., 14 bp ins./14 bp ins.). The details of mutant sequences are summarized in Extended Data Table 3. Wild-type and single homozygous fish for *hoxa13a* or *hoxa13b* were treated by PTU to inhibit pigmentation. The body size and length of mutant embryos are relatively normal at 72 hpf. *n* = 5 embryos for all genotypes. **b, f, j, n, r**, Bright field images of pectoral fins. Pectoral fins were detached from the body and photographed (Methods). *Hoxa13a*<sup>-/-</sup>,

*a13b*<sup>-/-</sup> double homozygous embryo shows 30% shorter pectoral fin fold compared to wild type (**r**, see also Extended Data Fig. 5). *n* = 5 embryos for all genotypes. **c, g, k, o, s**, *and1* *in situ* hybridization at 72 hpf. *Hox13* mutants show normal expression patterns, which indicates that fin fold development is similar to wild type in these mutants. *n* = 3 embryos for all genotypes. **d, h, l, p, t**, *shha* *in situ* hybridization at 48 hpf. *Hox13* mutants show a normal expression pattern that is related to relatively normal anteroposterior asymmetry of adult fin (Fig. 3, Extended Data Fig. 4 and Supplementary Information). *n* = 3 embryos for all genotypes. Scale bars are 1 mm (**a**), 200  $\mu$ m (**b, c**) and 100  $\mu$ m (**d**).

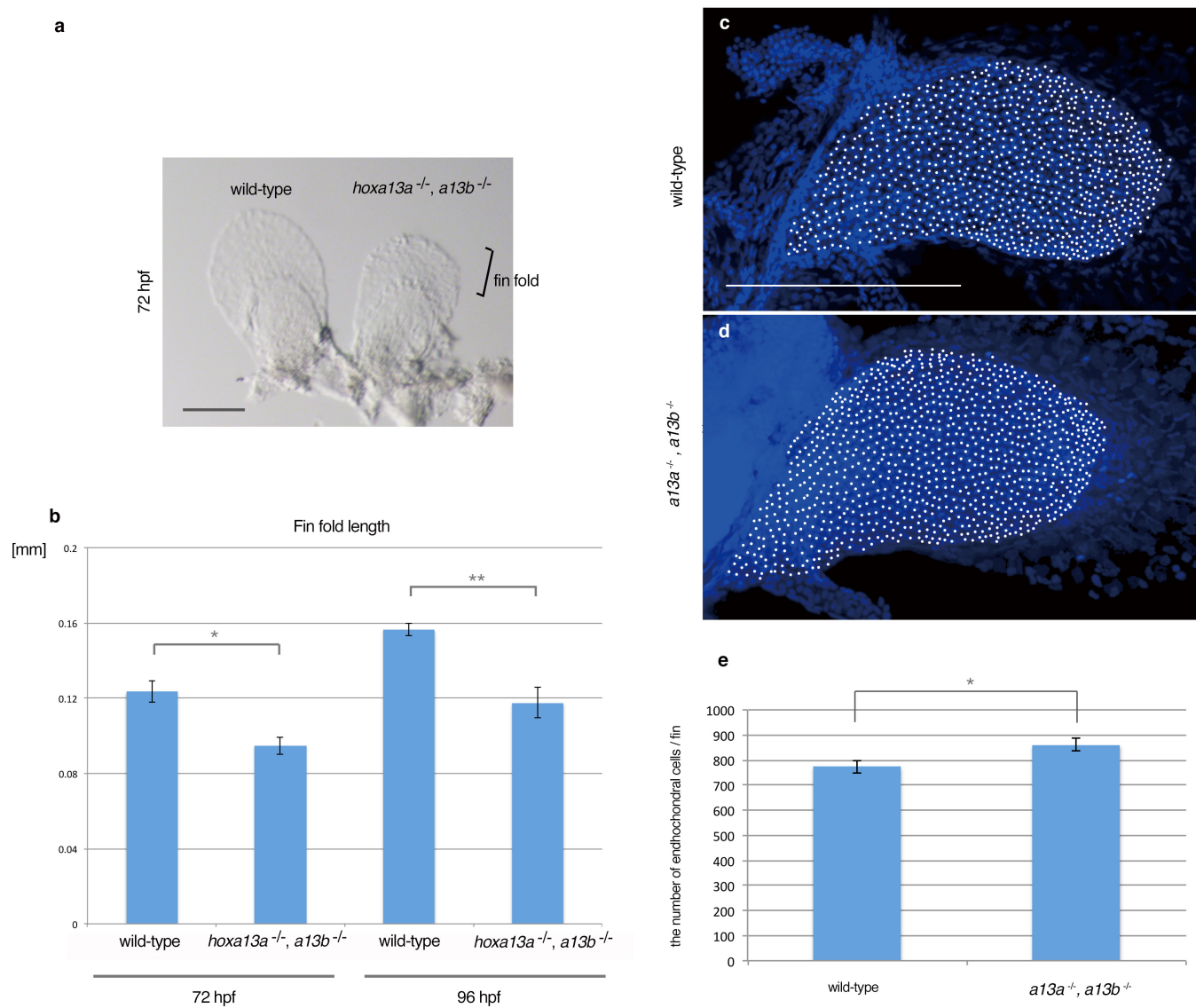


Extended Data Figure 4 | See next page for caption.

**Extended Data Figure 4 | Phenotype of adult *hox13* mutant fish.**

**a, c, e, g, i, k, m,** Whole body morphology of *hox13* deletion mutants were photographed at 4 months old; *hoxa13a*<sup>-/-</sup> (8 bp del./29 bp del.), *hoxa13b*<sup>-/-</sup> (4 bp del./14 bp ins.), *hoxd13a*<sup>-/-</sup> (5 bp ins./10 bp ins.), *hoxa13a*<sup>-/-</sup>, *hoxa13b*<sup>-/-</sup> double homozygous fish (8 bp del./29 bp del., 14bp ins./14 bp ins.) and triple knockout (**k, m**, mosaic for *hoxa13a*, *hoxa13b* and *hoxd13a*) fish (Methods). *n* = 3 fish for wild type, single and double mutants and *n* = 5 fish for triple mosaic mutants (same specimens were used as in Fig. 3). The details of mutant sequences are summarized in Extended Data Table 3. Each homozygous mutant fish shows normal morphology at 4 months old except for slightly short pectoral fin rays of *hoxa13a*<sup>-/-</sup> or *a13b*<sup>-/-</sup> single mutants. *Hoxa13a*<sup>-/-</sup>, *hoxa13b*<sup>-/-</sup> double homozygous fish shows a severe reduction of fin rays in pectoral, pelvic, dorsal and anal fins compared with wild type. The triple knockout (mosaic for *hoxa13a*, *hoxa13b* and *hoxd13a*) fish also showed a reduction in fin rays. Scale bar is 5 mm. Owing to the size of the adult fish, three different pictures for anterior, centre and posterior of the body were merged to make whole-body pictures. **b, d, f, h, j, l, n,** Bone staining pictures of mutant fish. The endochondral bones of pectoral fins are shown. Whereas single homozygous fish show relatively normal proximal radials (**b, d, f, h** and Fig. 3), double homozygous mutants show fused third and fourth

proximal radials (**j**). One triple knockout (mosaic for *hoxa13a*, *hoxa13b* and *hoxd13a*, 0, 25, 50%) fish had fused third and fourth proximal radials (**i**), but another triple knockout (0, 0, 0%) had more broken down proximal radials (**n**). *n* = 3 fish for wild type, single and double mutants and *n* = 5 fish for triple mosaic mutants (same specimens were used as in Fig. 3). The scale bar is 500  $\mu$ m. **o, p,** Examples of counting distal radials in wild-type and *hoxa13a*<sup>-/-</sup>, *hoxa13b*<sup>-/-</sup> double homozygous fish. First distal radials are not shown in CT segmentation because of a fusion with first fin ray. **q,** The number variation of distal radials in mutant fish. Multiple fins were investigated in wild type (25 fish/50 fins), *hoxa13a*<sup>-/-</sup> (4 bp del./4 bp del., 3 fish/6 fins), *hoxa13b*<sup>-/-</sup> (4 bp del./14 bp ins., 3 fish/6 fins), *hoxd13a*<sup>-/-</sup> (5 bp ins./17 bp del., 3 fish/6 fins), *hoxa13a*<sup>-/-</sup>, *hoxa13b*<sup>-/-</sup> double homozygous (8 bp del./29 bp del., 14 bp ins./14 bp ins., 3 fish/6 fins) and triple knockout (mosaic for *hoxa13a*, *hoxa13b* and *hoxd13a*) fish (five fish/10 fins). The number of distal radials increased to 10 and 13 in double and triple mutants, respectively. The difference in distal radial number between wild-type and double homozygous or wild-type and triple knockout fish (mosaic for *hoxa13a*, *hoxa13b* and *hoxd13a*) is statistically significant ( $P = 0.0014$  or  $P = 0.00001$ , respectively, *t*-test comparing the means, two-tailed distribution).



**Extended Data Figure 5 | Analysis of embryonic fin fold and endochondral disk in *hoxa13a*<sup>-/-</sup>, *hoxa13b*<sup>-/-</sup> embryos.** **a**, A bright field image of wild-type and *hoxa13a*<sup>-/-</sup>, *hoxa13b*<sup>-/-</sup> pectoral fins at 72 hpf. Pectoral fins were detached from the body and photographed (Methods). Scale bar is 150  $\mu$ m. **b**, The difference in fin fold length between wild-type and *hoxa13a*<sup>-/-</sup>, *hoxa13b*<sup>-/-</sup> embryos. The length of the fin fold was measured in wild-type ( $n=8$ ) and *hoxa13a*<sup>-/-</sup>, *hoxa13b*<sup>-/-</sup> double homozygous ( $n=5$ ) embryos at 72 hpf and 96 hpf (Methods). The length of the fin folds was decreased to about 70% of wild

type in double homozygous embryos (72 hpf;  $P=0.006$ , 96 hpf;  $P=0.004$ , *t*-test comparing the means, one-tailed distribution, see Source Data). The error bars indicate s.e.m. **c, d**, Images of DAPI staining of wild-type (c) and *hoxa13a*<sup>-/-</sup>, *hoxa13b*<sup>-/-</sup> mutant (d) pectoral fins captured by confocal microscopy. White circles indicate nuclei in the endochondral disks. Scale bar is 200  $\mu$ m. **e**, The average number of cells in the endochondral disk of wild-type and *hoxa13a*<sup>-/-</sup>, *hoxa13b*<sup>-/-</sup> mutant fins (see Methods and Source Data). The difference is statistically significant ( $P=0.041$  by Student's *t*-test, one-tailed distribution). The error bars indicate s.e.m.



**Extended Data Table 2 | PCR primers for CRISPR/Cas9 deletion, T7E1 assay, genotypes and gene cloning**

## CRISPR gRNA oligos

zebra *hoxa13a*\_gRNA1\_F  
 5'- ATTAATACGACTCACTATAGGGCAATCACAACCAGTGGAGTTTAGAGCTAGAAATAGC -3'  
 zebra *hoxa13a*\_gRNA2\_F  
 5'- ATTAATACGACTCACTATAGGCAGTAAAGACTCATGTCGGTTTAGAGCTAGAAATAGC -3'  
 zebra *hoxa13b*\_gRNA1\_F  
 5'- ATTAATACGACTCACTATAGGATATGAGCAAAAACAGTTTAGAGCTAGAAATAGC -3'  
 zebra *hoxa13b*\_gRNA2\_F  
 5'- ATTAATACGACTCACTATAGGACACTTCTGTTCTGGAGGTTTAGAGCTAGAAATAGC -3'  
 zebra *hoxd13a*\_gRNA1\_F  
 5'- ATTAATACGACTCACTATAGGCTCTGGCTCCTCACGTTAGAGCTAGAAATAGC -3'  
 zebra *hoxd13a*\_gRNA2\_F  
 5'- ATTAATACGACTCACTATAGGCGAACTCTTAAGCCAGCGTTAGAGCTAGAAATAGC -3'  
 zebra gRNA\_R  
 5'- AAAAGCACCAGCTCGGTGCCACTTTCAAGTTGATAACGGACTAGCCTATTAACTTGCTATTCTAGCTCTAAAAC -3'

## T7 assay primers

zebra *hoxa13a*\_Cont\_F  
 5'- CTGCAGCGGGTGATTCTG -3'  
 zebra *hoxa13a*\_Cont\_R  
 5'- CTCCTTACCGTCGGTTT -3'  
 PCR product: 810 bp  
 zebra *hoxa13b*\_Cont\_F  
 5'- GAAGCTTATCACTAGAACATTTACAGC -3'  
 zebra *hoxa13b*\_Cont\_R  
 5'- TTTTCTCAGGGCCTAAAGGT -3'  
 PCR product: 1089 bp  
 zebra *hoxd13a*\_Cont\_F  
 5'- AGCTGCCAATCACATGC -3'  
 zebra *hoxd13a*\_Cont\_R  
 5'- CGATTATAAATTCAAGTTGCTCTTAG -3'  
 PCR product: 823 bp

Genotype primers for single (*hoxa13a* or *a13b*) and double (*hoxa13a, a13b*) mutants

zebra *hoxa13a*\_8 bp del\_F  
 5'- GCCAAGGAGTTGCCTTGTA -3'  
 zebra *hoxa13a*\_8 bp del\_R  
 5'- TGACGACTTCCACACGTTTC -3'  
 PCR product: wild-type 231 bp, mutant (cut by Ava1) 111 +119 bp  
 zebra *hoxa13a*\_29 bp del\_F  
 5'- CAGGCAATAAGCGGGCCTT -3'  
 zebra *hoxa13a*\_29 bp del\_R  
 5'- GTGCAGTAGACCTGTCCGTT -3'  
 PCR product: wild-type 110 bp, mutant 81 bp  
 zebra *hoxa13b*\_14 bp ins\_F  
 5'- GATTGACCCGGTGATGTTTC -3'  
 zebra *hoxa13b*\_14 bp ins\_R  
 5'- TACACTGGTCGCAGCAAA -3'  
 PCR product: wild-type 98 bp, mutant (cut by Bcc1) 53 + 57 bp

## Cloning primers

Danio\_and1\_F  
 5'-ACCTGCTCCTGCTCCAGTTA -3'  
 Danio\_and1\_R  
 5'-CACATCCTTTGAGGGGAAA -3'

For synthesis of gRNAs, each forward primer and common reverse primer ('zebra gRNA\_R') were hybridized and used as templates. For genotype of single and double mutants, PCR products were treated by the enzymes indicated.

Extended Data Table 3 | List of *hox13* mutant sequences**a.***hoxa13a*

TCCAGGCAATAAGCGGGCCTTGGAGGCCCGACATGAGTCCTTACTGCCGATGGAGAGTTACCAACCGTGGAATCACAAACCGATGGATGGAAC	wild-type
TCCAGGCAATAAGCGGGCCTTGGAGGCCCGACATGAGTCCTTACTGCCGATGGAGAGTTACCAACCGTGGAATCACAAACCGATGGATGGAAC	-22 -7 = 29 bp deletion
TCCAGGCAATAAGCGGGCCTTGGAGGCCCGA-----GTCTTACTGCCGATGGAGAGTTACCAACCGTGGAATCACAAACCGATGGATGGAAC	-5 -3 = 8 bp deletion
TCCAGGCAATAAGCGGGCCTTGGAGGCCCGA-----GTCTTACTGCCGATGGAGAGTTACCAACCGTGGAATCACAAACCGATGGATGGAAC	-5 + 1 = 4 bp deletion

**b.***hoxa13b*

CTATGACAACGGTTGGATGATATGAGCAAAACATGGAAGG-----TACATGGACACTCTGTTCTGGAGAGGAGT	wild-type
CTATGACAACGGTTGGATGATATGAGCAAATGGAAGGATGGAGC ACATGGAAGG-----TACATGGACACTCTGTTCTGGAGAGGAGT (+1bp ins.)	14 bp insertion
CTATGACAACGGTTGGATGATATGAGCAA-----ATGGAAGG-----TACATGGACACTCTGTTCTGGAGAGGAGT	4 bp deletion

**c.***hoxd13a*

ATCCAATATGGCTGGCTCCTTCACGTTGGATGCCATT-----CGGTGAAGCCTCCA GCTGGCTTAAAGAGTTGCCTTTATCAAGG	wild-type
ATCCAATATGGCTGGCTCCTTCAC AAAAAAATGGCGTTGGATGCCATT-----CGGTGAAGCCTCCA G CCT CAGCTTAAAGAGTTGCCTTTATCAAGG	7 + 3 = 10 bp insertion
ATCCAATATGGCTGGCTCCTTCAC GGCT TTGGATGCCATT-----CGGTGAAGCCTCCA GCTGGCTTAAAGAGTTGCCTTTATCAAGG	5bp insertion
ATCCAATATGGCTGGCTCCTTCAC-----TTGGATGCCATT-----CGGTGAA-----GCTTAAGAGTTGCCTTTATCAAGG	-11 -6 = 17 bp deletion

**d.***hoxa13a*

TCCAGGCAATAAGCGGGCCTTGGAGGCCCGACATGAGTCCTTACTGCCGATGGAGAGTTACCAACCGTGGAATCACAAACCGATGGATGGAAC	wild-type	0%
TCCAGGCAATAAGCGGGCCTTGGAGGCCCGA-----GTCTTACTGCCGATGGAGAGTTACCAACCGTGGAATCACAA-----GTGGATGGAAC	-5 -3 = 8 bp deletion	100%

**e.***hoxa13b*

CTATGACAACGGTTGGATGATATGAGCAAAACATGGAAGG-----TACATGGACACTCTGTTCTGGAGAGGAGT	wild-type	0%
CTATGACAACGGTTGGATGATATGAGCAAATGGAAGGATGGAGC ACATGGAAGG-----TACATGGACACTCTGTTCTGGAGAGGAGT (+1bp ins.)	14 bp insertion	50%
CTATGACAACGGTTGGATGATATGAGCAA-----AA TTTTTGAGG-----TACATGGACACTCTGTTCTGGAGAGGAGT	-1 - 6 = 7 bp deletion	50%

**f.***hoxd13a*

ATCCAATATGGCTGGCTCCTTCACGTTGGATGCCATT-----CGGTGAAGCCTCCA GCTGGCTTAAAGAGTTGCCTTTATCAAGG	wild-type	0%
ATCCAATATGGCTGGCTCCTT-----TGGATGCCATT-----CGGTGAAGCCTCCA GCTGGCTTAAAGAGTTGCCTTTATCAAGG	6bp deletion	14.3%
ATCCAATATGGCTGGCTCCTCTGGCT CGTT TGGATGCCATT-----CGGTGAAGCCTCCA GCTGGCTTAAAGAGTTGCCTTTATCAAGG	4bp insertion	28.5%
ATCCAATATGGCTGGCTCCTCAG TCCAATG GTT TGGATGCCATT-----CGGTGAAGCCTCCA GCTGGCTTAAAGAGTTGCCTTTATCAAGG	8bp insertion	14.3%
ATCCAATATGGCTGGCTCCTCAG GCT CGTTGGATGCCATT-----CGGTGAAGCCTCCA GCTGGCTTAAAGAGTTGCCTTTATCAAGG	170bp deletion	14.3%
ATCCAATATGGCTGGCTCCTCAG TCCAATG GTT TGGATGCCATT-----CGGTGAAGCCTCCA GCTGGCTTAAAGAGTTGCCTTTATCAAGG	3bp insertion	14.3%
ATCCAATATGGCTGGCTCCTCAG TCCAATG GTT TGGATGCCATT-----CGGTGAAGCCTCCA -----GCTTAAGAGTTGCCTTTATCAAGG	+ 8 - 4 = 4bp insertion	14.3%

**g.**

Figure 3, Extended Data Fig.4a-p (4 months adult)

	<i>hoxa13a</i>	<i>hoxa13b</i>	<i>hoxd13a</i>
<i>hoxa13a</i> -/-	8 bp del. / 29 bp del.		
<i>hoxa13b</i> -/-		4 bp del. / 14 bp ins.	
<i>hoxd13a</i> -/-			5bp ins. / 10 bp ins.
double homo	8 bp del. / 29 bp del.	14 bp ins./ 14 bp ins.	
Triple KO1	0%	25%	50%
Triple KO2	0%	0%	0%

Extended Data Fig.3, 5 (embryo), Extended Data Fig.4q (adults for radial count)

	<i>hoxa13a</i>	<i>hoxa13b</i>	<i>hoxd13a</i>
<i>hoxa13a</i> -/-	4 bp del. / 4 bp del.		
<i>hoxa13b</i> -/-		4 bp del. / 14 bp ins.	
<i>hoxd13a</i> -/-			5bp ins. / 17 bp del.
double homo	8 bp del. / 29 bp del.	14 bp ins./ 14 bp ins.	

Frame-shift mutation alleles that were used for each experiment are listed. The top sequence in each column show wild type with gRNA sequence in red. Green is insertional and blue is substitutional mutations. **a.**, *hoxa13a* mutation patterns. Three types of mutations were used in this paper. Horizontal bars are deletional mutations. **b.**, *hoxa13b* mutation patterns. Sequences flanked by two gRNAs are abbreviated by black horizontal bars. Additional 1 bp is inserted at 3' side of the gRNA target side in '14 bp insertion'. **c.**, *hoxd13a* mutation patterns. Sequences flanked by two gRNAs are abbreviated by black horizontal bars. **d-f.**, Mutational patterns in a triple knockout (mosaic for *hoxa13b* and *hoxd13a*) fish that is shown in Fig. 3p-r are listed. Sequence flanked by two gRNAs are abbreviated by horizontal bars in **e** and **f**. Each *hox13* gene shows some different mutations indicating that this fish is highly mosaic. The percentage of mutant alleles was calculated from the result of deep sequencing (Fig. 3 and Extended Data Table 4). **g.**, Summary of genotype in all experiments. del. (deletion), ins. (insertion).

## Extended Data Table 4 | Genotyping of progeny from mutant crosses

**a**

<i>hoxa13a</i> <sup>+/−</sup> × <i>hoxa13a</i> <sup>+/−</sup>					
		+/-	-/-	Total	
Embryos (72 hpf)	9 (25.0%)	17 (47.2%)	10 (27.8%)	36	
Adult	9 (21.4%)	20 (47.6%)	13 (31%)	42	

<i>hoxa13b</i> <sup>+/−</sup> × <i>hoxa13b</i> <sup>+/−</sup>					
		+/-	-/-	Total	
Embryos (72 hpf)	8 (25.0%)	20 (62.5%)	12 (37.5%)	32	
Adult	20 (32.3%)	32 (51.6%)	10 (16.1%)	62	

<i>hoxd13a</i> <sup>+/−</sup> × <i>hoxd13a</i> <sup>+/−</sup>					
		+/-	-/-	Total	
Embryos (72 hpf)	8 (22.9%)	18 (51.4%)	9 (25.7%)	35	
Adult	5 (26.3%)	11 (57.9%)	3 (15.8%)	19	

**b**

<i>hoxa13a</i> <sup>+/−</sup> , <i>a13b</i> <sup>+/−</sup> × <i>hoxa13a</i> <sup>+/−</sup> , <i>a13b</i> <sup>+/−</sup> (72 hpf)					
<i>a13a</i>	<i>a13b</i>	+/-	-/-	Total	
+/-	20 (11.0%)	25 (13.7%)	10 (5.5%)	55 (30.2%)	
+/-	23 (12.6%)	50 (27.5%)	10 (5.5%)	83 (45.6%)	
-/-	6 (3.3%)	28 (15.4%)	10 (5.5%)	44 (24.2%)	
Total	49 (26.9%)	103 (56.6%)	30 (16.5%)	182 (100.0%)	

<i>hoxa13a</i> <sup>+/−</sup> , <i>a13b</i> <sup>+/−</sup> × <i>hoxa13a</i> <sup>+/−</sup> , <i>a13b</i> <sup>+/−</sup> (Adult)					
<i>a13a</i>	<i>a13b</i>	+/-	-/-	Total	
+/-	4	8	0	12 (22.2%)	
+/-	4	18	5	27 (50.0%)	
-/-	3	5	7	15 (27.8%)	
Total	11(20.4%)	31(57.4%)	12(22.2%)	54 (100.0%)	

**c**

	total adult fish	short finned fish	%
Negative control: Cas9 only	96	0	0.00
Cas9, <i>hoxa13b</i> and <i>d13a</i> gRNAs	161	7	4.35

**d**

Genotype of short fin fish (The percent of normal alleles are shown)

	#1	#2	#3	#4	#5	#6	#7
<i>hoxa13a</i>	20%	50%	0%	0%	25%	25%	0%
<i>hoxa13b</i>	20%	0%	25%	0%	0%	0%	0%
<i>hoxd13a</i>	100%	67%	50%	25%	30%	100%	0%

**a.** Breeding data in *hox13* single mutants. Single heterozygous fish were crossed with each other to obtain embryos and next generations. Embryos (72 hpf) or adult fish (3 months) were genotyped by T7E1 assay and sequenced. The number of each genotype and percentages are shown. The ratio of each genotype approximately follows Mendelian ratio. **b.** Breeding data for double *hoxa13* mutants. Double heterozygous fish (*hoxa13a*<sup>+/−</sup>, *hoxa13b*<sup>+/−</sup>) were crossed to obtain embryos and next generations. Embryos (72 hpf) or adult fish (three months) were genotyped by PCR followed by enzyme digestion (Methods) or sequencing. The number of each genotype and percentage are shown. The ratio of each genotype approximately follows Mendelian ratio. **c.** The efficiency of triple knockout (mosaic for *hoxa13a*, *hoxa13b* and *hoxd13a*) in zebrafish (See Methods). The number of normal adult fish and short-finned fish from negative control injection (Cas9 mRNA without gRNAs) or triple knockout injection (Cas9 mRNA with gRNAs) are shown. Genotypes for short-finned fish were calculated from deep sequencing of each allele and shown as a percentage of normal alleles in **d**.